Kinetic Anisotropy and Dendritic Growth in Electrochemical Deposition

D. Barkey, F. Oberholtzer, and Q. Wu
Department of Chemical Engineering, University of New Hampshire, Durham, New Hampshire 03824
(Received 9 June 1995)

It is shown that kinetic anisotropy stabilizes dendritic growth in electrochemical deposition of copper, and that in its absence the growth tips are unstable to splitting. The degree of anisotropy in the interfacial dynamics, which may be controlled through the chemistry of the electrolyte solution, was determined by the measurement of open-circuit potentials of single-crystal electrodes under nonequilibrium conditions. The experiments provide direct evidence that microscopic interfacial anisotropy in depositional growth stabilizes the dendritic morphology.

PACS numbers: 68.70.+w, 05.70.Ln, 81.10.Dn, 81.15.Pq

A central problem in the study of pattern formation is the origin of selection rules that lead to reproducible structures in nonequilibrium growth [1,2]. Much theoretical work has been directed to the question of whether interfacial anisotropy is a necessary condition for the formation of stable dendrites [3–11]. Experiments in fluid displacement have been put forward to provide physical evidence [12–14], but no depositional growth system has previously been reported in which interfacial kinetic parameters can be controlled. Here we present results for a driven-growth system, based on electrochemical deposition of copper by reduction of cupric ion in aqueous solution, in which the interfacial dynamics can be measured and varied to test the predictions of the theoretical models. We show that kinetic anisotropy in the microscopic dynamics of the interface stabilizes the dendritic morphology, and that in our experiments in its absence the growth tips are unstable to splitting.

A dendrite is a needle crystal characterized by its tip radius and growth velocity. Viewed in a moving reference frame, it maintains a constant shape. The shape and growth velocity of a dendrite must allow a self-consistent and stable solution of the transport equation subject to activation and capillary boundary conditions [1]. Based on the boundary-layer model, Ben-Jacob *et al.* proposed that anisotropy is required to stabilize the tip against splitting [3–5]. The same conclusion was reached with the geometric model [6] and solutions to the full diffusion problem [7–11]. Experiments with fluid displacement in the anisotropic Hele-Shaw cell, where the anisotropy is introduced by milling channels in one plate of the cell, provided additional support [12]. Buka and Palffy-Muhoray obtained a consistent result with liquid crystals in a Hele-Shaw cell, where the fluid viscosity is anisotropic [13]. While the models have been formulated for solidification from the melt, both the models and the experiments with fluid displacement have been cited as evidence of the role of anisotropy in crystallization generally.

The interpretation of results from Hele-Shaw cells was challenged by Couder *et al.*, who showed that stable parabolic fingers could be generated by the placement of a bubble on the tip [14]. They argued that it is the introduction of a length scale, the bubble diameter, that selects a stable tip. In addition, numerical simulation by Pines, Zlatkowski, and Chait [11] of the full dynamic problem without the steady state assumption showed selection of a stable tip without anisotropy.

Resolution of the issue requires a physical system in which deposition of a single material can be performed with and without interfacial anisotropy. Several studies have addressed the role of equilibrium interfacial anisotropy in dendritic solidification and precipitation by comparing the shape and growth velocity with the predictions of theoretical models [15–19]. Pairs of materials with contrasting surface-tension anisotropies, pivalic acid/succinonitrile [15,18], and pivalic acid/ammonium chloride [19] have also been examined. In part because of the restricted range of parameters, no strong conclusions can be made regarding a particular theoretical model, although there is evidence that the dendrite shape is independent of the magnitude of anisotropy for small values [15,19]. However, these studies do not apply directly here because none of the materials produce tip splitting, and the anisotropy is fixed for a given material.

Electrochemical deposition was introduced to the field of pattern formation as a means of producing a wide range of morphologies including tip splitting and dendritic branches as well as diffusion limited aggregates [20–23]. It was soon recognized that interfacial anisotropy could lead to a transition from tip splitting to dendritic growth as deposition parameters were varied [23]. In these investigations, however, the use of high-resistivity solutions forced the application of high field strengths, which mask the interfacial polarization. In electrochemical deposition from well-supported electrolyte solutions, where Ohmic dissipation is greatly reduced, the interface presents a substantial portion of the impedance, making the interfacial dynamics experimentally accessible.

To examine the role of interfacial dynamics and anisotropy in electrochemical deposition, we performed potential measurements on the metal-solution interface of copper single-crystal electrodes in supported solutions. Electrodes with orientations of (100), (110), and (111) were studied in a conventional three-electrode

 0031-9007/95/75(16)/2980(4)$06.00

electrochemical cell with a mercury/mercurous sulfate reference electrode. The composition of the electrolyte solution was $0.5M$ $CuSO_4/0.5M$ H_2SO_4 (sulfate solution) or $0.5M$ $CuCl_2/0.5M$ H_2SO_4 (chloride solution). Each electrode was polished mechanically with 0.05 μm alumina, electropolished in orthophosphoric acid, and degreased with benzene in a Soxhlet column. The electrodes were mounted on a single holder and brought into contact with the electrolyte. The holder was then withdrawn about 4 mm to form hanging menisci so that contact with the solution was confined to the polished faces.

When the sulfate solution was deaerated with nitrogen, the open-circuit potentials of the electrodes were stable and equal to -355 mV within the experimental uncertainty of 2 mV. When the solution was exposed to air, the (111) electrode became negative of the (100) and (110) electrodes by 5 or 6 mV consistent with the results of Jenkins and Bertocci [24]. In chloride solution, there was a transient beginning near -500 mV. Within 15 min, the potentials reached steady values, with the (111) electrode 15 to 18 mV negative of the other electrodes. Deaeration had no effect on the measurement. The magnitude of anisotropy is consistent with that reported by Bertocci, although in his solutions, prepared with cuprous ion, the (110) face behaved more like the (111) [25]. For comparison, we prepared a cuprous chloride solution consisting of $0.5M$ CuCl, $1.0M$ HCl, and $1.5M$ NaCl, and measured potentials in close agreement. The anisotropy in open-circuit potentials is much greater than in sulfate solution.

To determine the effect of interfacial properties on morphology, we formed copper electrodeposits from both solutions in the thin-layer cell shown in Fig. 1. The deposits were grown from the tip of an insulated copper wire in a 160 μm thick horizontal layer of electrolyte solution between glass plates 4 cm on a side. The plates rested in a Petri dish filled with solution up to the level of the space between the plates. The reference electrode and a circular anode 6 cm in diameter were placed in the pool of solution in the dish. The deposits were formed at a constant potential with respect to the mercury/mercurous sulfate reference electrode.

Representative deposits are shown in Fig. 2. In sulfate solution, the surfaces of the deposits were isotropic [Fig. 2(a)]. This solution corresponds to the first two entries in Table I, where the open-circuit potentials are isotropic for deaerated solution and only slightly anisotropic when exposed to air. The deposition cell is intermediate between the two since access by oxygen to the solution around the deposit is limited by diffusion. In the deposition experiments, the initially circular interface was unstable and developed tip-splitting fingers, which spread and shielded one another. At higher driving force there were more fingers, and they were narrower.

Deposition from chloride solution produced locally anisotropic features. This solution corresponds to the third and fourth entries in Table I in which the potentials are strongly anisotropic. At low driving force a faceted morphology was produced, while at high driving force, the aggregate was made up of fine dendrites with regular side branches [Fig. 2(b)].

The anisotropy that generates the difference in morphologies can be understood through an examination of the microscopic mechanism of deposition and the reactions that determine the open-circuit potentials in Table I [26]. The three species of copper present are the metal Cu, the cupric ion Cu^{2+}, and the cuprous ion Cu^{1+}. They are coupled by two elementary electrochemical reactions. The first involves only species in solution, and is therefore relatively insensitive to the crystalline orientation of the electrode [27]:

$$Cu^{2+} + e^- \Longleftrightarrow Cu^{1+}. \quad (1)$$

The second produces an atom on the surface, and can be expected to depend strongly on the surface orientation:

$$Cu^{1+} + e^- \Longleftrightarrow Cu. \quad (2)$$

Deposition is produced when reactions (1) and (2) are forced from left to right, so that the overall reaction is

$$Cu^{2+} + 2e^- \Longrightarrow Cu. \quad (3)$$

At the open-circuit potential, where no current is passed, equilibrium between the solution and the metal is approached by the progress of reactions (1) and (2) in opposite directions. Since our solutions were prepared with cupric ion only, equilibrium is obtained after contact with the metal by the progress of reaction (1) from left to right and by reaction (2) from right to left to produce cuprous ion,

$$Cu^{2+} + Cu \Longrightarrow 2Cu^{1+}. \quad (4)$$

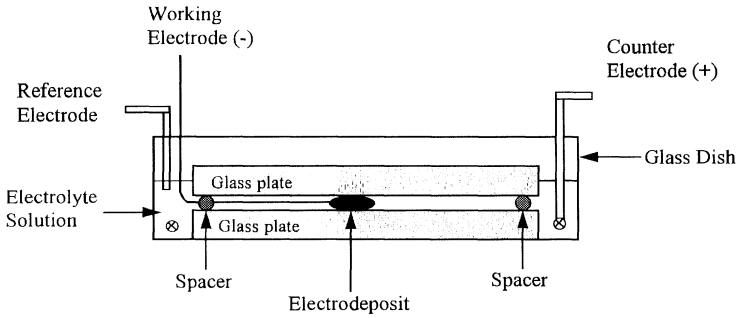

FIG. 1. Thin-layer electrochemical cell with reference electrode.

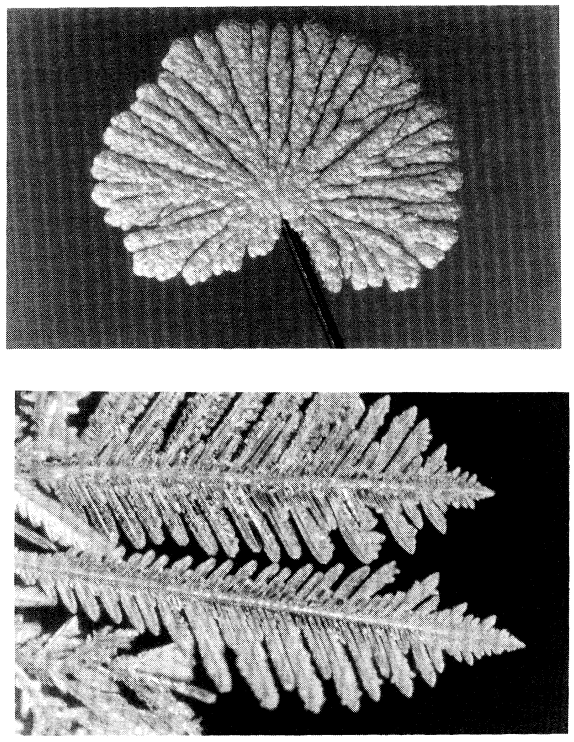

FIG. 2. Deposits formed by electrochemical deposition (a) from 0.5*M* $CuSO_4$/0.5*M* H_2SO_4 at 350 mV (frame width = 2.5 mm); and (b) from 0.5*M* $CuCl_2$/0.5*M* H_2SO_4 at 500 mV (frame width = 0.6 mm).

In sulfate solution the cuprous ion is unstable, and the equilibrium constant for reaction (4) is of the order 10^{-6} [26]. The deaerated solution comes into equilibrium with the metal after a very small fraction of the cupric ions has been consumed, and the different crystal faces then adopt the same potential [24]. The interfacial free energy, which may be anisotropic, has no effect on the equilibrium potentials because the electrodes are planar.

Dissolved oxygen oxidizes the cuprous ion to give cupric ion, so that if the solution is not deaerated, reaction (4) does not come into equilibrium, which depends on the crystallographic plane that is exposed to the solution [24]. Since this anisotropy appears only at disequilibrium, it is kinetic in character.

In chloride solution, the cuprous ion is stabilized by formation of complexes, and it is the predominant species at equilibrium [25,26]. Since our solution is prepared with the cupric ion, it is not at equilibrium with the metal, and reaction (4) continues until most of the cupric ion is consumed, even if the solution is deaerated. The resulting nonequilibrium potentials depend on the face exposed to the solution.

The potential adopted by the metal when reaction (4) is out of equilibrium is a mixed potential determined in part by the kinetics of reactions (1) and (2). Reaction (1) involves only ions in solution, and thus should be less sensitive to the surface orientation than reaction (2), which produces an atom on the surface [27]. We therefore expect processes controlled by reaction (1) to be isotropic and those controlled by reaction (2) to be anisotropic. In deposition from sulfate solution, where the cuprous ion is unstable, the rate-limiting step is reaction (1) [28,29]. As a result, the interfacial dynamics of deposition are isotropic, and tip-splitting growth is observed. In chloride solution, where the cuprous ion is stabilized, reaction (2) is controlling, the interfacial dynamics are anisotropic, and dendritic growth is observed. The solution prepared with the cuprous ion also produced faceted deposits. However, we have focused on cupric chloride for the purpose of comparison with cupric sulfate.

To investigate the effect of anisotropy on the selected velocity, we found a time-averaged growth velocity by measuring the time required for the aggregates to reach a diameter of 1.75 mm. Figure 3 shows a plot of average velocity versus overpotential (applied potential minus open-circuit potential). The overpotentials were varied from 220 to 630 mV, and the velocities fell between 0.02 and 10 μm/s, a range of 3 orders of magnitude. The log-log plot gives a slope of 4.7 for the sulfate solution and 4.3 for the chloride solution. At a given overpotential the velocity in the chloride solution was about 80 times greater than the velocity in the sulfate solution.

The global deposition rate is equal to the cell current divided by twice the Faraday constant, since the solutions were made with divalent copper. The cell current ranged from 0.2 to 2.8 mA and was larger for the chloride solution. However, the contrast in current at a given overpotential was much smaller, never more than twofold, than the contrast in velocity. Transport limitations on the global deposition rate therefore cannot account for the enormous velocity contrast. The critical difference between the solutions is in the interfacial processes, which determine the distribution of local deposition rates.

TABLE I. Open-circuit potentials of single-crystal electrodes vs Hg/Hg_2SO_4.

Solution	Potential (mV) (100)	(110)	(111)
0.5*M* $CuSO_4$/0.5*M* H_2SO_4 deaerated	−355	−354	−355
0.5*M* $CuSO_4$/0.5*M* H_2SO_4 in air	−364	−365	−370
0.5*M* $CuCl_2$/0.5*M* H_2SO_4 in air, 0 min	−480	−492	−503
0.5*M* $CuCl_2$/0.5*M* H_2SO_4 in air, 15 min	−380	−377	−395
0.5*M* CuCl/1.0*M* HCl/1.5*M* NaCl in air, 15 min	−542	−556	−564

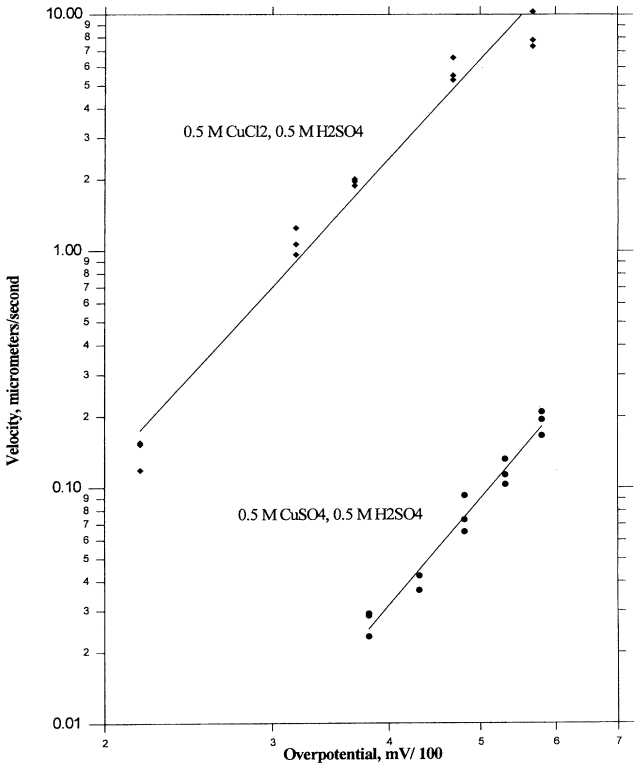

FIG. 3. Velocity versus driving force. 0.5M $CuSO_4$/0.5M H_2SO_4 (●), 0.5M $CuCl_2$/0.5M H_2SO_4 (◆).

In our experiments, dendrites grow much faster than tip-splitting fingers. Following the analogy to phase transitions advanced by Ben-Jacob *et al.* [30], we suppose that the system adopts the fastest growing morphology. If the cell current is limited in part by ion transport, a faster growing morphology sustains a higher current, or global flux, because it sweeps through a greater volume of solution in unit time [31]. We conjecture that the faster morphology is selected in transport-limited growth because it sustains a higher global flux and, hence, a more rapid approach to equilibrium. When interfacial anisotropy is introduced to the copper electrochemical deposition system, a fast growing dendritic morphology becomes available. In its absence, the system is confined to the slower isotropic morphology.

We thank Dr. Peter Garik for many helpful discussions. This work was supported by the National Science Foundation under Grant No. CTS-9306837.

[1] E. Ben-Jacob and P. Garik, Nature (London) **343**, 523 (1990).
[2] L. M. Sander, Nature (London) **322**, 789 (1986).
[3] E. Ben-Jacob, N. D. Goldenfeld, J. S. Langer, and G. Schon, Phys. Rev. Lett. **51**, 1930 (1983); Phys. Rev. A **29**, 330 (1984).
[4] E. Ben-Jacob, N. D. Goldenfeld, B. G. Kotliar, and J. S. Langer, Phys. Rev. Lett. **53**, 2110 (1984).
[5] D. A. Kessler, J. Koplick, and H. Levine, Phys. Rev. A **30**, 3161 (1984).
[6] R. C. Brower, D. A. Kessler, J. Koplick, and H. Levine, Phys. Rev. Lett. **51**, 1111 (1983); Phys. Rev. A **29**, 1335 (1984).
[7] D. A. Kessler and H. Levine, Phys. Rev. A **33**, 7867 (1986).
[8] D. I. Meiron, Phys. Rev. A **33**, 2704 (1986).
[9] Y. Saito, G. Goldbeck-Wood, and H. Mueller-Krumbhaar, Phys. Rev. Lett. **58**, 1541 (1987).
[10] Y. Miyata, M. E. Glicksman, and S. H. Tirmizi, J. Cryst. Growth **110**, 683 (1991).
[11] V. Pines, M. Zlatkowski, and A. Chait, Phys. Rev. A **42**, 6137 (1990).
[12] E. Ben-Jacob, R. Godbey, N. D. Goldenfeld, J. Koplick, H. Levine, T. Mueller, and L. M. Sander, Phys. Rev. Lett. **55**, 1315 (1985).
[13] A. Buka and P. Palffy-Muhoray, Phys. Rev. A **36**, 1527 (1987).
[14] Y. Couder, O. Cardoso, D. Dupuy, P. Tavernier, and W. Thom, Europhys. Lett. **2**, 437 (1986).
[15] M. E. Glicksman and N. B. Singh, J. Cryst. Growth **98**, 277 (1989).
[16] E. R. Rubenstein and M. E. Glicksman, J. Cryst. Growth **112**, 84 (1991).
[17] A. Dougherty, J. Cryst. Growth **110**, 501 (1991).
[18] M. Muschol, D. Liu, and H. Z. Cummins, Phys. Rev. A **46**, 1038 (1992).
[19] A. Dougherty and A. Gunawardana, Phys. Rev. E **50**, 1349 (1994).
[20] R. M. Brady and R. C. Ball, Nature (London) **309**, 225 (1984).
[21] M. Matsushita, M. Sano, Y. Hayakawa, H. Honjo, and Y. Sawada, Phys. Rev. Lett. **53**, 286 (1984).
[22] Y. Sawada, A. Dougherty, and J. P. Gollub, Phys. Rev. Lett. **56**, 1260 (1986).
[23] D. Grier, E. Ben-Jacob, R. Clark, and L. M. Sander, Phys. Rev. Lett. **56**, 1264 (1986).
[24] L. H. Jenkins and U. Bertocci, J. Electrochem. Soc. **112**, 517 (1965).
[25] U. Bertocci, J. Electrochem. Soc. **113**, 604 (1966).
[26] *The Encyclopedia of the Electrochemistry of the Elements,* edited by A. J. Bard and H. Lund (Marcel Dekker, New York, 1973), p. 384.
[27] J. O'M. Bockris and G. Razumney, Electroanal. Chem. Int. Electrochem. **41**, 1 (1973).
[28] E. Mattson and J. O'M. Bockris, Trans. Faraday Soc. **55**, 1586 (1959).
[29] O. R. Brown and H. R. Thirsk, Electrochim. Acta **10**, 383 (1965).
[30] E. Ben-Jacob, P. Garik, T. Mueller, and D. Grier, Phys. Rev. A **38**, 1370 (1988).
[31] D. Barkey, P. Garik, E. Ben-Jacob, B. Miller, and B. Orr, J. Electrochem. Soc. **139**, 1044 (1990).

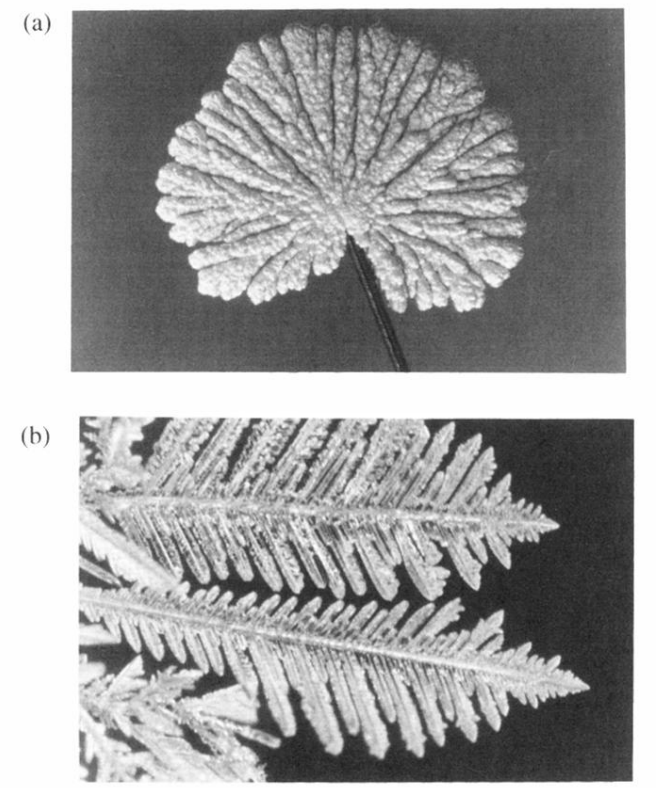

FIG. 2. Deposits formed by electrochemical deposition (a) from 0.5*M* $CuSO_4$/0.5*M* H_2SO_4 at 350 mV (frame width = 2.5 mm); and (b) from 0.5*M* $CuCl_2$/0.5*M* H_2SO_4 at 500 mV (frame width = 0.6 mm).